# Increased DC trafficking to lymph nodes and contact hypersensitivity in junctional adhesion molecule-A–deficient mice

Maria Rosaria Cera, … , Alberto Mantovani, Elisabetta Dejana

**Article**   **Vascular biology**

Junctional adhesion molecule-A (JAM-A) is a transmembrane adhesive protein expressed at endothelial junctions and in leukocytes. In the present work, we found that DCs also express JAM-A. To evaluate the biological relevance of this observation, *Jam-A*$^{-/-}$ mice were generated and the functional behavior of DCs in vitro and in vivo was studied. In vitro, *Jam-A*$^{-/-}$ DCs showed a selective increase in random motility and in the capacity to transmigrate across lymphatic endothelial cells. In vivo, *Jam-A*$^{-/-}$ mice showed enhanced DC migration to lymph nodes, which was not observed in mice with endothelium-restricted deficiency of the protein. Furthermore, increased DC migration to lymph nodes was associated with enhanced contact hypersensitivity (CHS). Adoptive transfer experiments showed that JAM-A⁻deficient DCs elicited increased CHS in *Jam-A*$^{+/+}$ mice, further supporting the concept of a DC-specific effect. Thus, we identified here a novel, non-redundant role of JAM-A in controlling DC motility, trafficking to lymph nodes, and activation of specific immunity.

**Find the latest version:**

https://jci.me/21231/pdf

# Increased DC trafficking to lymph nodes and contact hypersensitivity in junctional adhesion molecule-A–deficient mice

Maria Rosaria Cera,[1] Annalisa Del Prete,[2,3] Annunciata Vecchi,[2] Monica Corada,[1,2]
Ines Martin-Padura,[1] Toshiyuki Motoike,[4] Paolo Tonetti,[2] Gianfranco Bazzoni,[2] William Vermi,[5]
Francesca Gentili,[5] Sergio Bernasconi,[2] Thomas N. Sato,[4] Alberto Mantovani,[2,6]
and Elisabetta Dejana[1,2,7]

[1]Department of Vascular Biology, Italian Foundation for Cancer Research (FIRC) Institute of Molecular Oncology, Milan, Italy. [2]Department of Immunology and Cell Biology, Mario Negri Institute for Pharmacological Research, Milan, Italy. [3]Section of Clinical Biochemistry, University of Bari, Bari, Italy. [4]University of Texas Southwestern Medical Center at Dallas, Dallas, Texas, USA. [5]Department of Pathology, University of Brescia, Brescia, Italy. [6]Centro di Eccellenza per l'Innovazione Diagnostica e Terapeutica Institute of General Pathology, Faculty of Medicine, University of Milan, Milan, Italy. [7]Department of Biomolecular and Biotechnological Sciences, School of Sciences, University of Milan, Milan, Italy.

**Junctional adhesion molecule-A (JAM-A) is a transmembrane adhesive protein expressed at endothelial junctions and in leukocytes. In the present work, we found that DCs also express JAM-A. To evaluate the biological relevance of this observation, *Jam-A*^–/– mice were generated and the functional behavior of DCs in vitro and in vivo was studied. In vitro, *Jam-A*^–/– DCs showed a selective increase in random motility and in the capacity to transmigrate across lymphatic endothelial cells. In vivo, *Jam-A*^–/– mice showed enhanced DC migration to lymph nodes, which was not observed in mice with endothelium-restricted deficiency of the protein. Furthermore, increased DC migration to lymph nodes was associated with enhanced contact hypersensitivity (CHS). Adoptive transfer experiments showed that JAM-A–deficient DCs elicited increased CHS in *Jam-A*^+/+ mice, further supporting the concept of a DC-specific effect. Thus, we identified here a novel, non-redundant role of JAM-A in controlling DC motility, trafficking to lymph nodes, and activation of specific immunity.**

## Introduction

Junctional adhesion molecule-A (JAM-A) is a 32-kDa transmembrane glycoprotein present in endothelial cells, epithelial cells, platelets, and leukocytes. In the endothelium and several types of epithelia, JAM-A is located at intercellular junctions and codistributes with tight junction components (1). Other members of the JAM family (JAM-B and JAM-C) have been recently identified (2, 3). These molecules have a more restricted cell distribution but the same localization at tight junctions (4–6).

The extracellular segment of JAM-A comprises two Ig-like domains, an amino terminal (VH type) and a carboxyl terminal (C2 type) fold, respectively. In solution, a recombinant soluble protein, which corresponds to the whole extracellular domain of JAM-A, binds in a homophilic manner, supporting the idea that JAM-A may mediate homotypic cell-to-cell adhesion (7). X-ray structure analysis suggests that JAM-A forms parallel and noncovalent homodimers, which might expose at the cell surface an adhesive interface for homophilic interactions (8).

Due to its junctional distribution, JAM-A may control transendothelial migration of leukocytes. We found that an anti–JAM-A mAb (BV11) was able to reduce infiltration of both monocytes and polymorphonuclear cells in in vivo models of inflammation in mice (1, 9).

The mechanism of action of JAM-A in promoting cell transmigration remains undefined. It has been suggested that it may have a role in binding leukocytes and in directing their transmigration through endothelial junctions. JAM-A was found to link leukocyte integrin αL-β2 (10), but homophilic binding of endothelial and leukocytic JAM-A may also occur. More recent data (11) show that endothelial JAM-A can reorganize at junctions during leukocyte transmigration, creating a transient ring around transmigrating leukocytes. This suggests that JAM-A may actively promote the passage of the cells through the endothelial monolayer, possibly creating a tunnel-like structure at endothelial junctions.

DCs play a key role in the activation of specific immunity (12), and trafficking to secondary lymphoid organs is crucial for their function. In the present paper we report that DCs express JAM-A. To assess the role of this protein in DC migration and in the activation of T cell responses, *Jam-A*^–/– mice were generated. JAM-A–deficient mice showed increased in vitro and in vivo migration of DCs and increased contact hypersensitivity (CHS). Genetic analysis revealed that the role of JAM-A in DC trafficking is independent of its expression in the endothelium. Thus, JAM-A expression has a negative role in the regulation of DC migration to lymph nodes and activation of specific immunity.
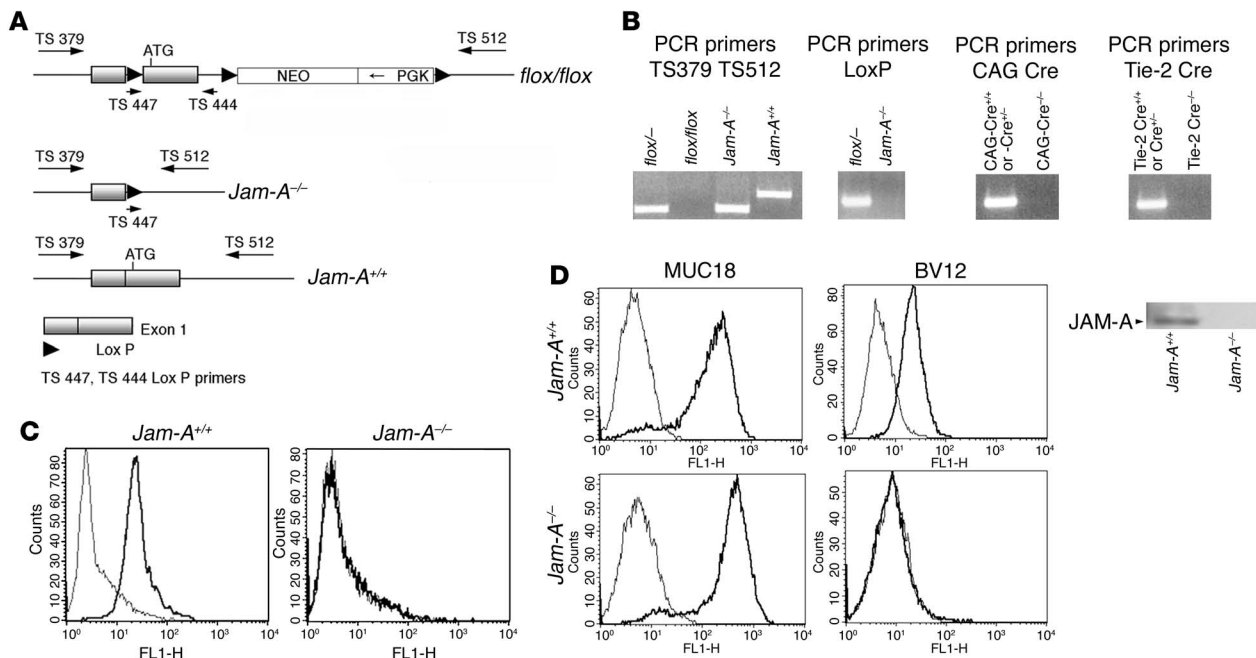
## Results

*Generation of Jam-A*^–/– *mice.* *Jam-A*^–/– mice were produced by generating a floxed *Jam-A* allele and by crossing these animals with *CAG-Cre* mice (13). A targeting vector was designed so that a LoxP site and a floxed pGK-neo resistance cassette were inserted into the 5′ UTR region and into intron 1 of the *Jam-A* gene, respectively (Figure 1A).

---

**Figure 1**
Characterization of *Jam-A*⁻/⁻ and endothelial *Jam-A*⁻/⁻ mice. (**A**) The targeted allele containing 3 LoxP sites (*flox/flox*), the excised allele (*Jam-A*⁻/⁻), and the WT allele (*Jam-A*⁺/⁺) are shown. (**B**) Genomic PCR of murine tail biopsies. To identify *Jam-A*⁻/⁻ mice obtained from interbreeding of heterozygous mice, the combination of CAG–Cre-F, CAG–Cre-R, TS379, TS512, TS447, and TS444 LoxP primers was used. To identify endothelial *Jam-A*⁻/⁻ mice, the combination of Tie-2 Cre, TS379, and TS512 primers was used. TS379 and TS512 generate a 500-bp product for minus allele, an 800-bp product for WT allele, and a 3,000-bp product (absence of band) for flox allele. (**C**) FACS analysis of JAM-A on mouse leukocytes isolated from peritoneal cavities 24 hours after injection of thioglycollate. (**D**) Expression of JAM-A on endothelial cells derived from lungs of *Jam-A*⁺/⁺ and *Jam-A*⁻/⁻ animals evaluated by FACS, immunoprecipitation, and Western blot analysis with mAb BV12. In **C** and **D**, gray lines represent negative controls obtained using the secondary Ab alone.

Interbreeding of heterozygous mice for the *Jam-A*⁻ allele generated heterozygous and homozygous offspring in the correct Mendelian ratios. DNA isolated from tail biopsies was used for genotyping the animals. Different combinations of flox JAM-A and/or *Jam-A*⁻ alleles were identified by PCR using primers TS512 and TS379 and LoxP primers TS447 and TS444 as shown in Figure 1B. The absence of JAM-A was confirmed by FACS analysis of leukocytes (Figure 1C), Western blot, FACS analysis of endothelial cells (Figure 1D), and histological analysis of different organs (Figure 2). At autopsy, mutant mice did not show significant alterations in organ development or morphology. The number of circulating platelets, lymphocytes, neutrophils, and monocytes was not significantly changed in *Jam-A*⁻/⁻ animals compared with *Jam-A*⁺/⁺ animals (not shown). In addition, the pattern of the vasculature (mesenteric, ear skin) in the adult was not significantly different in *Jam-A*⁻/⁻ mice compared with *Jam-A*⁺/⁺ mice as evaluated by the mean diameter of the vessels or number of branches per length unit (not shown) (14). Basal and induced vascular permeability in the ear, measured as described (15), was not significantly increased in *Jam-A*⁻/⁻ mice compared with *Jam-A*⁺/⁺ mice.

To study the role of JAM-A specifically expressed on endothelial cells in regulating DC migration, a genetic approach was used. We crossed (see Methods) mice containing two floxed *JAM-A* alleles with heterozygous transgenic mice (*Jam-A*⁺/⁻) expressing Cre under the endothelium-specific promoter of *Tie-2* (16). By immunofluorescence staining (Figure 2, A–C), JAM-A was undetectable in both vascular and lymphatic endothelial cells, but it retained its normal expres-

sion in epithelial cells. The identification of *Tie-2 Cre*–positive genotypes was done using Tie-2 Cre primers as shown in Figure 1B. To distinguish between the heterozygous *Jam-A*^flox/⁻ and *Jam-A*^flox/⁺ mice, the primers TS379 and TS512 were used.

*Increased migratory capacity of Jam-A*⁻/⁻ *DCs.* Previous studies have shown that JAM-A is expressed in myelomonocytic cells as well as in endothelial cells, where it was originally identified (1). These observations were extended to murine (Figure 3A) and human (not shown) DCs. Murine bone marrow–derived DCs (BM-DCs) expressed JAM-A and its levels were not substantially affected by exposure to TNF-α, a classic maturation signal (Figure 3A). It was therefore important to investigate whether JAM-A deficiency affected DC function. Immature and mature *Jam-A*⁻/⁻ DCs were similar to *Jam-A*⁺/⁺ DCs in terms of membrane phenotype (Figure 3B), mixed lymphocyte response (Figure 3C), and FITC-dextran uptake (Figure 3D).

To further investigate whether there were alterations of endogenous DCs in secondary lymphoid tissue, the phenotype of lymph node cells and DC subsets in lymph nodes were analyzed. As shown in Figure 4A, *Jam-A*⁺/⁺ and *Jam-A*⁻/⁻ mice have a comparable pattern of lymphoid cell populations (Figure 4A) and subsets (Figure 4B) of myeloid, lymphoid, and plasmacytoid DCs.

The migratory properties of *Jam-A*⁻/⁻ DCs were then investigated. As shown in Figure 5A, in a Transwell assay, *Jam-A*⁻/⁻ DCs showed normal chemotactic responsiveness to chemokines that are preferentially active on immature (CCL3) and mature (CCL19) DCs.

Transendothelial migration was then investigated. As shown in Figure 5B, *Jam-A*⁻/⁻ and *Jam-A*⁺/⁺ DC migration was equally low
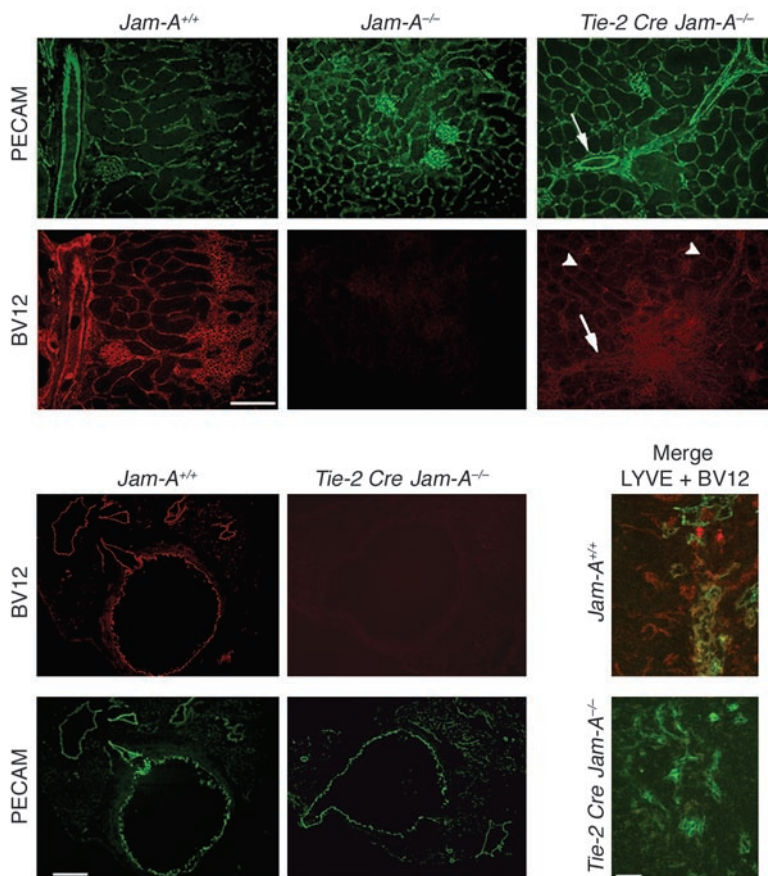
**Figure 2**
Histological analysis of *Jam-A⁻/⁻* and endothelial *Jam-A⁻/⁻* mice. (**A**) Immunofluorescence staining of serial cryosections of *Jam-A⁺/⁺*, *Jam-A⁻/⁻*, and endothelial *Jam-A⁻/⁻* (*Tie-2 Cre Jam-A⁻/⁻*) kidneys using anti-PECAM and anti–JAM-A (BV12) Ab's. All sections show positive staining for PECAM (both controls and mutants), while JAM-A staining is undetectable in all type of tissues in *Jam-A⁻/⁻* mice. Note that endothelial cells from *Tie-2 Cre Jam-A⁻/⁻* animals are negative for JAM-A staining (arrow). The arrowheads indicate that JAM-A staining on the epithelium of the tubuli is still detectable. Staining is weaker compared with *Jam-A⁺/⁺* mice since the peritubular capillaries are negative. Scale bar: 200 μm. (**B**) Immunostaining of serial cryosections of aorta from *Jam-A⁺/⁺* and *Tie-2 Cre Jam-A⁻/⁻* mice, using anti-PECAM and anti–JAM-A (BV12) Ab's. Vascular endothelial JAM-A is undetectable in *Tie-2 Cre Jam-A⁻/⁻* aorta. Scale bar: 200 μm. (**C**) Cryosections of *Jam-A⁺/⁺* and *Tie-2 Cre Jam-A⁻/⁻* lymph nodes were double stained for LYVE (in green), a marker of lymphatic endothelial cells, and for JAM-A (in red). In *Jam-A⁺/⁺* mice, the colocalization of JAM-A and LYVE is evident; this was not observed in *Tie-2 Cre Jam-A⁻/⁻* animals. Scale bar: 50 μm.

through blood microvascular endothelium (1G11 cells). In contrast, when mouse lymphatic endothelial cells (MELCs) were used, *Jam-A⁻/⁻* DCs showed a significant increase in transendothelial migration compared with *Jam-A⁺/⁺* cells in both the apical-to-basal and the basal-to-apical directions.

When a more refined gold-track system was used to measure cell migration, *Jam-A⁻/⁻* DCs showed a marked increased in random motility compared with *Jam-A⁺/⁺* cells (Figure 5C). When a JAM-A–blocking mAb was added to *Jam-A⁺/⁺* mature DCs (mDCs) and immature DCs (iDCs), we observed a significant increase in random motility. The area covered by migrating cells in a typical experiment was 112.11 ± 16.56 μm² (mean ± SEM) for control iDCs and 337.31 ± 10.56 μm² for BV11-treated iDCs (20 μg/ml); 104.96 ± 13.96 μm² for control mDCs and 598.27 ± 17.36 μm² for BV11-treated mDCs. No significant effect was observed after adding an anti-PECAM/CD31 blocking mAb: 100.90 ± 10.01 μm², mean ± SEM, for controls and 115.10 ± 21.05 μm² for Ab-treated (20 μg/ml) iDCs; 120.23 ± 18.01 μm² and 150.41 ± 15.33 μm² for control and Ab-treated mDCs, respectively.

We then investigated whether expression of membrane proteins relevant to DC trafficking (including the other two members of the JAM family, JAM-B and JAM-C) was altered in BM-DCs (Figure 6A) and lymphoid cells (Figure 6B). No significant difference was observed between *Jam-A⁺/⁺* and *Jam-A⁻/⁻* cells.

These results show that *Jam-A⁻/⁻* DCs present increased migratory capacity, but only in selected in vitro systems (gold-track random migration and transmigration across lymphatic endothelium). It was therefore important to assess the actual in vivo relevance of

the increased migratory ability of *Jam-A⁻/⁻* DCs. The FITC painting, contact sensitization assay was used to assess cutaneous DC migration in *Jam-A⁻/⁻* mice. FITC was applied to the skin of *Jam-A⁺/⁺* and *Jam-A⁻/⁻* mice and the number of FITC/CD11c double-positive cells recovered from the draining lymph nodes was evaluated by FACS analysis. As shown in Figure 7A, the number of FITC⁺/CD11c⁺ cells was significantly increased in *Jam-A⁻/⁻* mice compared with *Jam-A⁺/⁺* mice.

To study the role of JAM-A specifically expressed on endothelial cells in regulating DC migration and trafficking to lymph nodes, the FITC painting assay was used with *Tie-2 Cre Jam-A⁻/⁻* mice. In these animals, in contrast to the *CAG-Cre Jam-A⁻/⁻* mice, there was no significant increase in DC migration to lymph nodes compared with *Jam-A⁺/⁺* mice (Figure 7B); in fact there was a small but consistent decrease.

*Defective CHS in Jam-A⁻/⁻ mice.* Previous work has shown that alterations in DC trafficking to lymph nodes are associated with defective activation of specific immunity (17, 18). It was therefore of interest to assess the capacity of *Jam-A⁻/⁻* mice to mount specific immune responses. *Jam-A⁻/⁻* mice were studied in a CHS model with oxazolone (OXA) as sensitizing agent (see Methods). Figure 8A shows the response of *Jam-A⁺/⁺* and *Jam-A⁻/⁻* mice sensitized on day 0 and challenged 5 days later. *Jam-A⁻/⁻* mice displayed increased ear swelling compared with *Jam-A⁺/⁺* mice at peak time (24 hours); swelling persisted up to 96 hours. To elucidate the specific role of *Jam-A⁻/⁻* DCs in the CHS response in comparison to other cell types, DCs derived from bone marrow of either *Jam-A⁺/⁺* or *Jam-A⁻/⁻* mice were loaded in vitro with the antigen 2,4-dinitro-
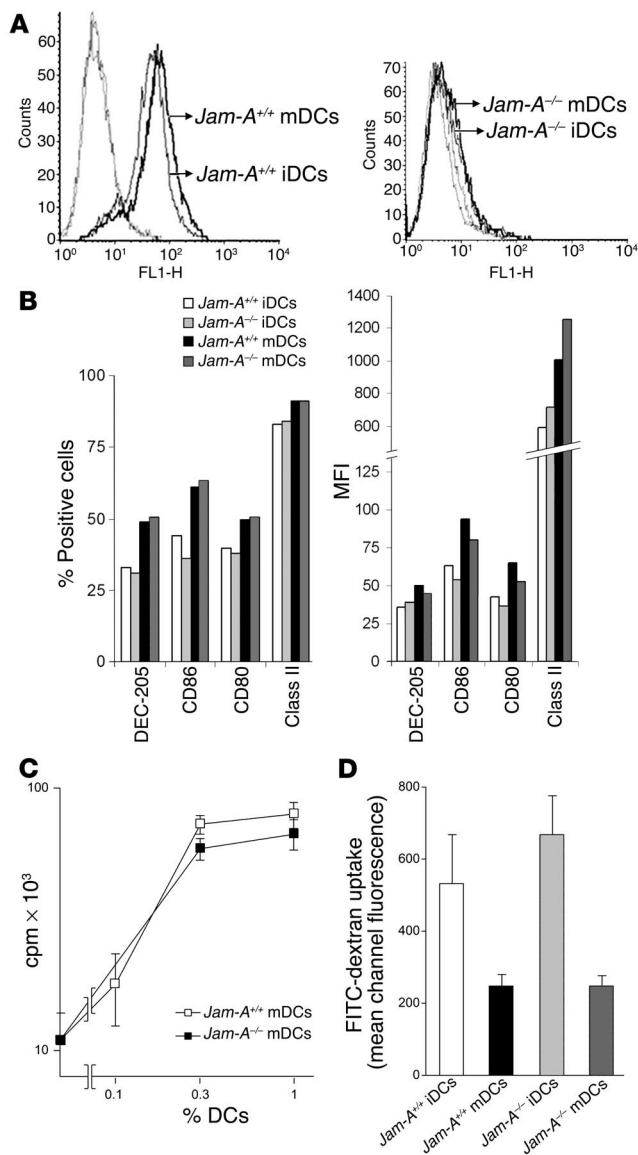
**Figure 3**
Characterization of DCs from *Jam-A⁺/⁺* and *Jam-A⁻/⁻* mice. CD34⁺ bone marrow precursor cells were used to generate iDCs and mDCs in vitro, and these were functionally characterized as detailed in Methods. (**A**) JAM-A expression on *Jam-A⁺/⁺* and *Jam-A⁻/⁻* iDCs and mDCs. Unlabeled lines correspond to staining with an irrelevant mAb of an identical isotype. (**B**) Membrane phenotype of iDCs and mDCs from *Jam-A⁺/⁺* and *Jam-A⁻/⁻* mice. Percentage and mean fluorescence intensity (MFI) of positive cells are shown. (**C**) Mixed lymphocyte response performed in the presence of different numbers of mDCs from *Jam-A⁺/⁺* and *Jam-A⁻/⁻* mice. mDCs are most effective in mixed lymphocyte response, and for simplicity only data with mDCs are shown in the Figure. iDCs from *Jam-A⁺/⁺* and *Jam-A⁻/⁻* mice did not differ in inducing mixed lymphocyte response (data not shown). (**D**) Uptake of FITC-dextran as evaluated by FACS analysis. Data in **B** are of one representative experiment out of five performed. Data in **C** and **D** are mean ± SEM of one representative experiment out of three performed in triplicate.

a pivotal role in the enhanced CHS observed in JAM-A–deficient mice. The specific response was not observed when the challenge was performed with the different antigen OXA (data not shown).

*Phenotype and count of DCs in tissues.* To exclude that the enhanced DC migration and CHS response shown in *Jam-A⁻/⁻* mice was due to an altered number and phenotype of DCs in the skin and in the lymph nodes, we analyzed skin sections and inguinal lymph nodes of *Jam-A⁺/⁺* and *Jam-A⁻/⁻* mice.

Histological analysis of inguinal lymph nodes from *Jam-A⁻/⁻* mice showed an architecture of the parenchyma comparable to *Jam-A⁺/⁺* organs (not shown), with the presence of multiple cortical lymphoid nodules along with an expanded paracortical T cell area (Figure 9A) densely populated by MHC class II⁺ DCs (Figure 9A, insert).

JAM-A expression was evaluated in lymph node and skin sections of *Jam-A⁺/⁺* mice by immunohistochemistry. JAM-A was strongly expressed on sinus macrophages (Figure 9B, asterisk) and in the paracortex on endothelial cells of high endothelial venules (Figure 9, B and C, arrowheads) and DCs (Figure 9C, arrow). No reactivity was observed on lymphoid cells (Figure 9, B and C). DCs of superficial lymph nodes include resident and migratory subsets. The latter are represented primarily by the nodal counterpart of skin-derived Langerhans cells (LCs). Due to its role in DC migration from the periphery to lymph nodes, JAM-A expression was

benzene sulfonic acid (DNBS) and inoculated into *Jam-A⁺/⁺* recipient mice (Figure 8B). Five days later mice were challenged with the antigen 2,4-dinitrofluorobenzene. Mice that had received DNBS-loaded *Jam-A⁻/⁻* DCs showed a significant increase in ear swelling. These results demonstrate that JAM-A deficiency specifically in DCs results in enhanced CHS response to DNBS and support the hypothesis that increased migration of DCs to lymph nodes plays

**Figure 4**
Analysis of lymph nodes. (**A**) FACS analysis of different populations of cells from inguinal lymph nodes from *Jam-A⁺/⁺* and *Jam-A⁻/⁻* mice (percentage and MFI). (**B**) DC subsets were characterized in peripheral lymph nodes from *Jam-A⁺/⁺* and *Jam-A⁻/⁻* mice. CD11c⁺ DCs were gated and stained for CD11b and CD8α. Myeloid DCs (M-DCs) are expressed as the percentage of CD11b⁺/CD8α⁻, and lymphoid DCs (L-DCs) are expressed as the percentage of CD11b⁻/CD8α⁺ DCs within the CD11c⁺ population. Plasmacytoid DCs (P-DCs) were identified as B220⁺ cells within a CD11c⁺/CD11b⁻ gated population. The same number of plasmacytoid DCs was found in *Jam-A⁺/⁺* and *Jam-A⁻/⁻* mice when B220⁺/GR1⁺ DCs were considered to be part of the CD11c⁺/CD11b⁻ gated population.
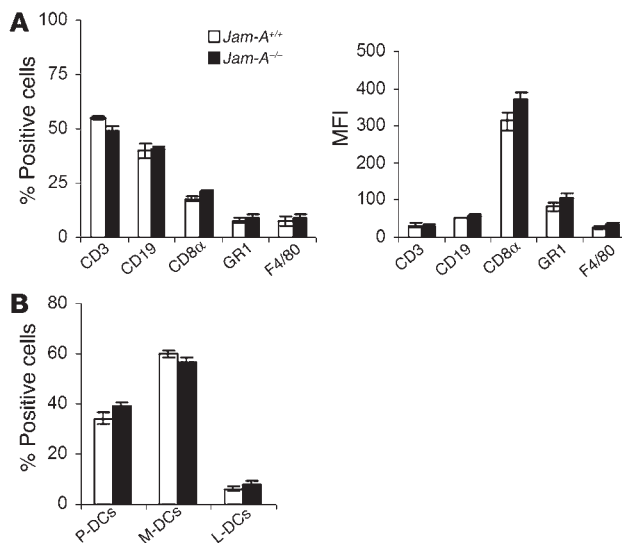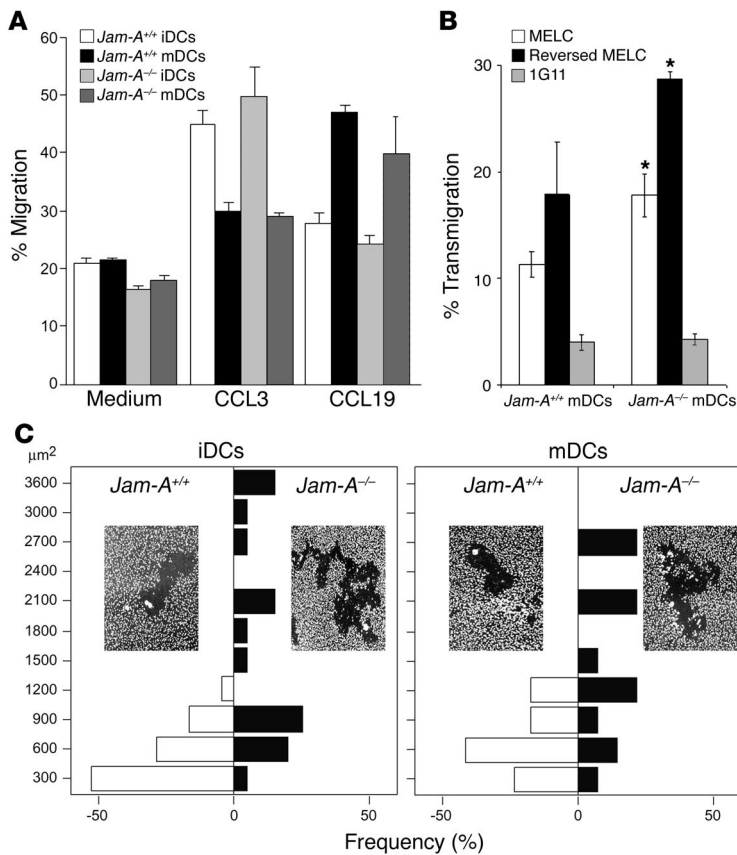
**Figure 5**
JAM-A expression and in vitro DC migration. (**A**) Chemotaxis of iDCs and mDCs was evaluated using the Transwell system. Data are presented as percent migration, calculated as described in Methods. Data are mean ± SEM of triplicates from a typical experiment out of three performed. (**B**) Basal transmigration of *Jam-A*^{+/+} and *Jam-A*^{–/–} mDCs across monolayers of vascular (1G11 cells) or lymphatic (MELCs) endothelial cells grown on the upper or lower side (reversed MELCs) of the filter (see Methods). Data, presented as percent transmigration, are mean ± SEM of triplicates from a typical experiment out of three performed. *$P < 0.01$ by paired Student's $t$ test comparing transmigration of *Jam-A*^{+/+} and *Jam-A*^{–/–} mDCs through MELCs. (**C**) Distribution of particle-free areas in random migration. Each bar represents the percentage of cells that have migrated over the indicated particle area in one representative experiment out of three performed. In this experiment the mean ± SEM of the particle area covered by migrating cells was 378 ± 46 μm² for *Jam-A*^{+/+} iDCs ($n = 25$ cells), 1,511 ± 249 μm² for *Jam-A*^{–/–} iDCs ($n = 20$ cells), 541 ± 79 μm² for *Jam-A*^{+/+} mDCs ($n = 17$ cells), and 1,448 ± 217 μm² for *Jam-A*^{–/–} mDCs ($n = 14$ cells).

evaluated in normal skin sections. A weak and diffuse JAM-A positivity was observed in the epidermis as previously reported (1). Due to this pattern of reactivity, we were unable to correctly decipher JAM-A expression on epidermal LCs. In the dermis (Figure 9D), *Jam-A*^{+/+} cells were represented by keratinocytes of the pilar follicle, endothelium of dermal vessels, and scattered dermal cells with stellate/dendritic morphology (Figure 9D, insert). JAM-A reactivity was absent in lymph nodes and cutaneous sections from *Jam-A*^{–/–} mice (not shown).

Skin sections were immunostained for anti–MHC class II molecules to identify LCs in the epidermis. Similarly to *Jam-A*^{+/+} animals (not shown), MHC class II[+] LCs from *Jam-A*^{–/–} mice were regularly distributed along the epidermis and exhibited normal morphology with fine and long dendrites (Figure 9E). In addition, LCs correctly expressed their specific marker Langerin (Figure 9E, insert). The density of LCs was evaluated in skin sections and the number of MHC-II[+] LCs was normalized to the number of DAPI[+] basal keratinocytes present in the same fields. No significant differences were observed in the number of LCs between *Jam-A*^{+/+} and *Jam-A*^{–/–} mice: the mean number of LCs/100 basal keratinocytes was 9.9 ± 3.1 in *Jam-A*^{+/+} animals and 9.7 ± 2.2 in *Jam-A*^{–/–} animals (mean ± SEM of 20 sections examined, $P = 0.32$ by Student's $t$ test).

Twenty-four hours after FITC labeling of the skin, green fluorescent cells were evaluated in lymph node sections from *Jam-A*^{+/+} and *Jam-A*^{–/–} mice by immunofluorescence microscopy. In *Jam-A*^{+/+} mice, green fluorescent cells were mainly located in the paracortical area and the majority of them expressed JAM-A (Figure 9F). In accordance with their LC origin, green fluorescent cells also expressed Langerin (Figure 9G) in both *Jam-A*^{+/+} and *Jam-A*^{–/–} mice.

## Discussion
This paper reports novel observations on the role of JAM-A in DC functional responses. We first found that DC cells express JAM-A on their surface. *Jam-A*^{–/–} DCs showed an unexpected selective increase in random migration and transmigration across lymphatic endothelial cells. Moreover, *Jam-A*^{–/–} mice showed increased localization to lymph nodes of skin DCs and enhanced CHS. Furthermore, in adoptive transfer experiments, *Jam-A*^{–/–} DCs showed an increased capacity to activate a CHS reaction. Thus JAM-A plays a nonredundant role in tuning DC trafficking and subsequent activation of specific immunity.

The increased in vitro and in vivo migration of DCs in *Jam-A*^{–/–} mice was unexpected. Previous in vitro and in vivo studies based on an anti–JAM-A mAb suggested that this molecule may facilitate monocyte and neutrophil transmigration and recruitment at sites of injury (9). However, in in vitro experiments, the mAb was directed to endothelial cells and not to leukocytes. In this paper we report that increased migration to lymph nodes was not observed in mice with endothelium-restricted deficiency, which actually showed a small but consistent reduction in lymph node homing, supporting the idea of a positive role of endothelial JAM-A in promoting cell extravasation. In addition, we have unpublished data showing that neutrophil infiltration in a model of peritoneal inflammation is reduced in *Jam-A*^{–/–} animals, consistent with the results obtained with the blocking mAb.

All together, these results suggest that JAM-A expressed in different cellular compartments may exert different and divergent influences and that the increased DC trafficking to lymph nodes observed in gene-targeted mice may be the net result of an alge-
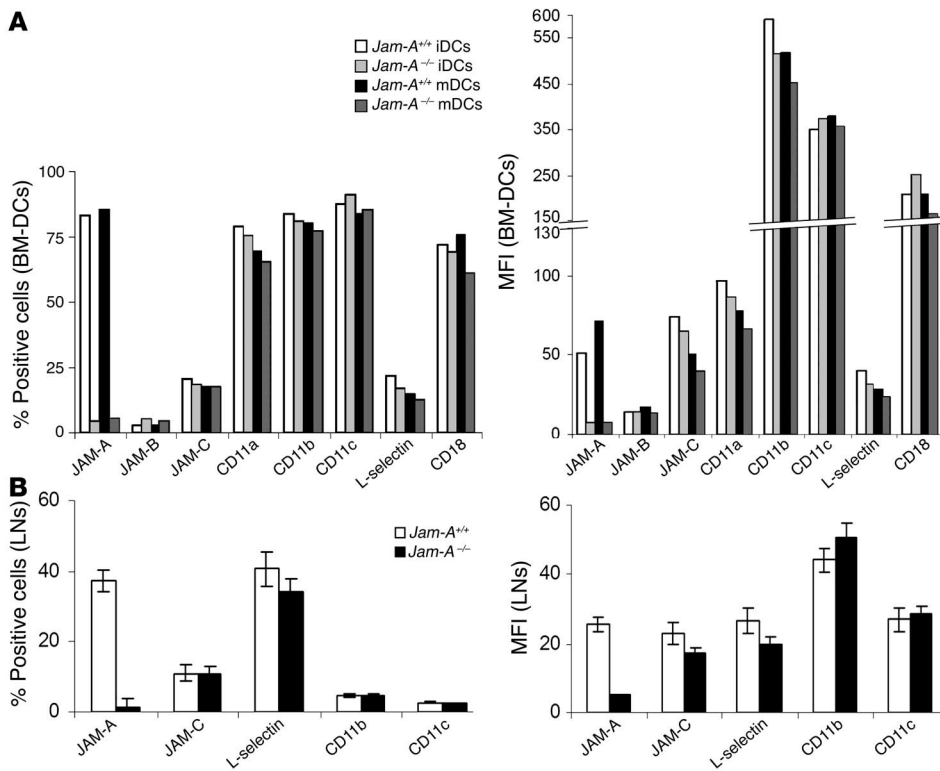
**Figure 6**
Expression of molecules involved in leukocyte traffic. (**A**) FACS analysis (percentage and MFI) of traffic molecules in BM-DCs from *Jam-A+/+* and *Jam-A–/–* mice. (**B**) Analysis of traffic molecules (percentage and MFI) in cells derived from inguinal lymph nodes of *Jam-A+/+* and *Jam-A–/–* mice. Data in **A** and **B** are from one representative experiment out of three performed.

braic sum of negative and positive effects of JAM-A. The mechanism of endothelium-independent promotion of DC trafficking to lymph nodes in *Jam-A–/–* mice remains to be fully elucidated.

Results of our gold-track experiments support the idea that JAM-A may limit random DC motility, while this effect is overcome when cells are activated by strong chemotactic agents (see Figure 5A). Transmigration through lymphatic but not blood endothelium is increased in *Jam-A–/–* DCs in vitro. Lymphatics allow dynamic interchanges of solutes and cells from lymph to tissues and vice versa. Consistent with this property, these cells present weak intercellular junctions with a specific molecular organization (19–21). This may explain why DCs migrate more efficiently through lymphatic cells than blood endothelial cells and why the effect of JAM-A inactivation may be more evident in this system. Other possible explanations such as altered expression of chemokines seem unlikely, since the lymphatic endothelial cell line used in this work produces relatively low amounts of CCL21 and CCL19 by ELISA assay and Affymetrix gene chip array analysis

(unpublished results). Moreover, JAM-A did not affect responsiveness to CCR7 ligands (see Figure 5A).

At a molecular level, JAM-A can bind through its cytoplasmic tail different intracellular proteins containing PDZ domains. These include ZO-1, CASK, afadin/AF6, and the PAR3-PAR6-aPKC complex (22–26). ZO-1, CASK, and afadin promote the anchorage of JAM-A to actin microfilaments (27–29), and this effect may be important in the dynamic assembly and disassembly of the actin cytoskeleton during cell migration. In addition, the PAR3-PAR6-aPKC complex controls activation of glycogen synthase kinase-3β, which may regulate stability of microtubules and single cell motility (30). It is possible that inactivation of the *Jam-A* gene causes uncontrolled activation/inhibition of these systems, leading to increased random cell migration.

In conclusion, in this paper we report for the first time a specific phenotype of *Jam-A–/–* animals. The data presented underline the complexity of the role of this molecule in regulating leukocyte traffic (31). JAM-A may exert different, and in some cases contrasting,

**Figure 7**
Increased in vivo migration of cutaneous DCs in *Jam-A–/–* mice. (**A**) Time course of recruitment of FITC+/CD11c+ DCs in lymph nodes (LN) following FITC skin painting. Results represent the mean ± SEM of a single experiment (seven mice per group) out of four performed (*$P < 0.01$, **$P < 0.001$ by Student's *t* test). The percentages of FITC+/CD11c+ DCs in lymph nodes were 1.0 ± 0.14 for *Jam-A+/+* mice and 0.8 ± 0.12 for *Jam-A–/–* mice at time 0; 2.76 ± 0.45 for *Jam-A+/+* mice and 5.01 ± 1.09 for *Jam-A–/–* animals at 6 hours, and 2.28 ± 0.28 and 4.94 ± 0.46 for *Jam-A+/+* and *Jam-A–/–* mice, respectively, at 24 hours. (**B**) Recruitment of FITC+/CD11c+ DCs in lymph nodes of *Tie-2 Cre Jam-A–/–* mice 24 hours after FITC skin painting. Results are mean ± SEM of one representative experiment (eight mice per group) out of three performed.
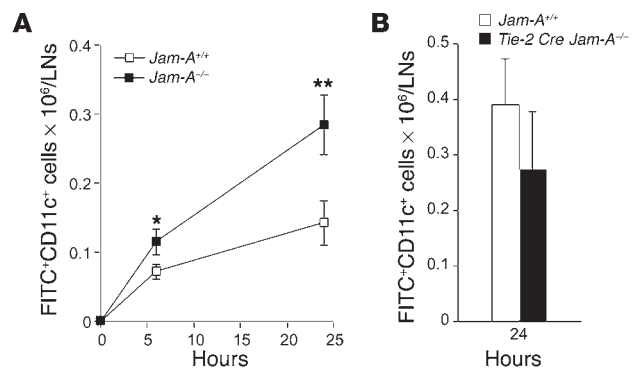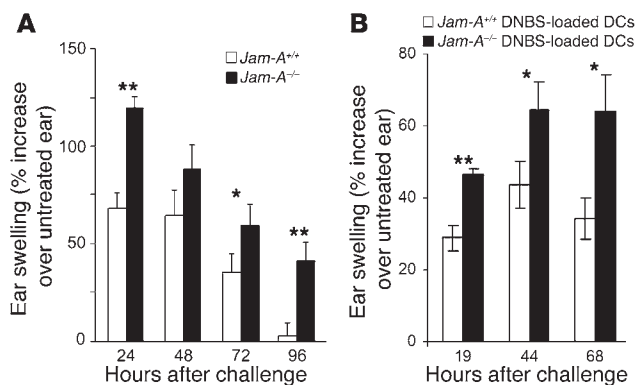
**Figure 8**

Increased CHS response in *Jam-A−/−* mice. (**A**) Animals were sensitized with OXA on their shaved abdominal skin and 5 days later were challenged on the right ear. Ear swelling was measured and expressed as percent increase over controls (left ear was painted with vehicle alone). The control mean values ± SEM were comparable: $23.86 \times 10^{-2} \pm 0.46 \times 10^{-2}$ mm for *Jam-A+/+* mice and $23.50 \times 10^{-2} \pm 0.28 \times 10^{-2}$ mm for *Jam-A−/−* mice. The values reported in the figure are mean ± SEM (8 mice per group) of one representative experiment out of three performed (*$P \leq 0.05$ and **$P < 0.01$ by Student's *t* test). (**B**) *Jam-A+/+* mice were immunized by subcutaneous injection of DNBS-loaded DCs obtained from *Jam-A+/+* or *Jam-A−/−* mice (see Methods). Mice were challenged 5 days later by ear painting with DNFB. Figures represent the percent increase of ear swelling over controls. Mean values ± SEM (8 mice per group) of one representative experiment out of three performed are shown (*$P \leq 0.05$ and **$P < 0.01$ by Student's *t* test). Mean ± SEM of vehicle-treated ears was comparable between both groups ($22.63 \times 10^{-2} \pm 0.26 \times 10^{-2}$ mm for *Jam-A+/+* and $22.25 \times 10^{-2} \pm 0.16 \times 10^{-2}$ mm for *Jam-A−/−* mice).

activities in different cell types. In DCs, JAM-A controls and limits cell motility while at endothelial cell junctions it may regulate and increase cell transmigration.

The proper localization of antigen-loaded DCs to secondary lymphoid organs is critical for an optimal activation of specific immunity (17, 18). The increased migration of DCs to lymph nodes in *Jam-A−/−* mice was associated with increased CHS. Therefore, targeting JAM-A in an appropriate cellular context may represent a strategy to modulate activation of immune responses.

## Methods

*Construction of the Jam-A−/− transgene and production of Jam-A−/− mice.* To construct the targeting vector, three LoxP sites were inserted in the *Jam-A* gene: a LoxP site into the 5′ UTR region of exon 1 and a pGK-neo resistance cassette flanked by two other LoxP sites in opposite orientation into intron 1. *Jam-A−/−* mice were generated by crossing *Jam-Aflox/flox* mice with *CAG-Cre* animals (13). To identify the *CAG-Cre* alleles, the primers CAG–Cre-F (5′-CCAAAATTT-GCCTGCATTACCGGTCGATGC-3′) and CAG–Cre-R (5′-AGCGCCGTA-AATCAATCGATGAGTTGCTTC-3′) were used in PCR, generating an 800-bp product. Different combinations of WT, flox JAM-A, and *Jam-A−* alleles were identified by PCR using primer TS379 (5′-CCTCTCTTTTCACCAATCGGA-3′) and the antisense TS512 (5′-TCTTCTTCAGACGCCGAACCT-3′), which generate a 500-bp product for *Jam-A−* allele, an 800-bp product for WT allele, and a 3,000-bp product (showing no band) for flox allele. To distinguish between homozygous *Jam-A−/−* and and heterozygous flox JAM-A/*Jam-A−* alleles, the LoxP primers TS447 (5′-CGTATAATGTATGCTATACGAAG-3′) and the antisense TS444 (5′-GAGGTAGGGTCACAGATCACC-3′) were used (350-bp product in the presence of flox allele).

Endothelial *Jam-A−/−* mice were obtained as previously described (14). For the identification of the *Tie-2 Cre* gene, the F-Tie-2 Cre primer (5′-CCCT-GTGCTCAGACAGAAATGAGA-3′) and the antisense primer Cre− (5′-CCAGCAGGCGCACCATTGCCCCTG-3′) were used in PCR, generating a 500-bp product. The Tie-2 Cre transgenic mice were a kind gift of Masashi Yanagisawa (University of Texas Medical Center) (16).

Procedures involving animals and their care conformed to institutional guidelines in compliance with national (4D.L. N.116, G.U., suppl. 40, 18-2-1992) and international law and policies (EEC Council Directive 86/609, OJ L 358, 1, 12-12-1987; NIH Guide for the Care and Use of Laboratory Animals, US National Research Council 1996). All efforts were made to minimize the number of animals used and their suffering.

*Cells and flow cytometry.* *Jam-A+/+* and *Jam-A−/−* endothelial cells were isolated from lungs and cultured as described in previous publications (32, 33). The endothelial nature of the cells was confirmed by FACS analysis and immunofluorescence with S-Endo-1/MUC18 (34, 35), VE-cadherin (rat mAb BV13) (36), PECAM (rat mAb Mec 13.3) (37), and other endothelial markers (not shown). Fluorescence flow cytometric analysis was performed with a FACStar Plus apparatus (BD Biosciences — Immunocytometry Systems) as previously described (35), using an FITC-conjugated donkey anti-rat Ab (Jackson ImmunoResearch Laboratories) as secondary Ab. JAM-A expression was analyzed using the anti–JAM-A mouse mAb BV12, as previously described (1).

MELCs were isolated from hyperplastic vessels (of liver and diaphragm) that were induced by intraperitoneal injection of incomplete Freund's adjuvant (38). These cells are positive for lymphatic markers such as VEGFR-3 (Santa Cruz Biotechnology Inc.) and podoplanin (a kind gift of Dontscho Kerjaschki, University of Vienna, Vienna, Austria), and junction markers such as JAM-A and ZO-1 (Zymed Laboratories Inc.) (see Supplemental Figure 1 and Supplemental Table 1; supplemental material available at http://www.jci.org/cgi/content/full/114/5/729/DC1). Other Ab's used to characterize the cells (see Supplemental Table 1) were LYVE (a kind gift of E. Ruoslahti, Cancer Research Center, The Burnham Institute, La Jolla, California, USA, and K. Alitalo, Biomedicum Helsinki, Helsinki University Central Hospital, Helsinki, Finland), JAM-C (a kind gift of B. Imhof, University of Geneva, Geneva, Switzerland), occludin (Zymed Laboratories Inc.), N-cadherin, and DSK (Ch1) (39) from BD Biosciences — Pharmingen.

For DC culture, 8- to 12-week-old *Jam-A+/+* and *Jam-A−/−* male mice were used. Mouse DCs were generated from mouse CD34+ bone marrow cells as previously described (40). Cells were characterized in terms of (a) membrane phenotype, (b) pinocytosis, and (c) mixed lymphocyte response on day 9 (40). Membrane phenotype was determined by expression of: DEC-205, identified by Ab HB-290 from the American Type Culture Collection (ATCC); CD86 (Ab HB-253, ATCC); I-A (anti-mouse MHC class II clone 2G9, BD Biosciences — Pharmingen); and CD80 (clone 1G10, BD Biosciences — Pharmingen). Where specified, DCs were cultured with TNF-α (20 ng/ml) for the last 24 hours of culture.

Other rat anti-mouse Ab's used to characterize DCs or secondary lymphoid tissues were: anti-CD18 (GAME-46, ATCC), anti-CD3 (145-2C11, ATCC), anti-CD19 (1D3, ATCC), allophycocyanin-conjugated (APC-conjugated) and FITC-conjugated anti-CD11b (M1/70, ATCC), PE-conjugated anti-CD11c (HL3, ATCC), PerCP-Cy5.5–conjugated anti–Gr-1 (RB6-8C5, ATCC), FITC-conjugated anti-CD45/B220 (RA3-6B2, ATCC), APC-conjugated anti-CD8α (clone 53-6.7, BD Biosciences — Pharmingen), anti-CD11a (Tib-217, ATCC), anti–L-selectin (HB-132, ATCC), and anti-F4/80 (HB-198, ATCC). Rabbit anti-mouse JAM-B was a kind gift of Steve Rosen (University of California, San Francisco, California, USA).

Immunoprecipitation and Western blot on cell extracts were performed as previously described (22).
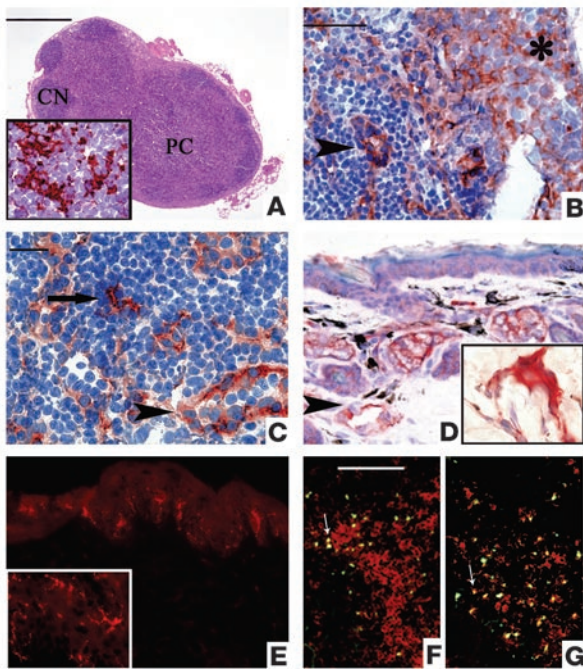
**Figure 9**
Morphology, JAM-A expression, and DC distribution in lymph node and skin sections. (**A**) H&E staining of a lymph node section from a *Jam-A*−/− mouse displays normal architecture including cortical lymphoid nodules (CN) and an expanded paracortical area (PC); PC is populated by DCs, highlighted by their strong expression of MHC class II molecule (inset). (**B**) Expression of JAM-A in a lymph node section from a *Jam-A*+/+ mouse is evident in sinus macrophages (asterisk), high endothelial venules (arrowheads in **B** and **C**), and DCs in the paracortex (**C**, black arrow). (**D**) In normal skin, a diffuse JAM-A expression is observed in epidermal and pilar keratinocytes, in endothelial cells of dermal vessels (arrowhead), and in scattered fusate/stellate dermal cells (inset). (**E**) A skin section from a *Jam-A*−/− mouse illustrates the regular distribution of MHC class II+ LCs; LCs display an evident dendritic morphology with fine and long dendrites, and express Langerin (insert). (**F** and **G**) Sections from an inguinal lymph node obtained after FITC skin painting display green-dotted FITC+ cells in the paracortex that coexpress JAM-A (**F**, arrow) and Langerin (**G**, arrow). MHC class II+ and JAM-A+ cells were detected by immunoperoxidase technique as seen in **A** (inset), **B**, **C**, and **D**. Immunofluorescence staining was used to detect JAM-A+ cells (red cells in **F**), MHC class II+ LCs (red cells in **E**), and Langerin+ LCs (red cells, inset in **E**; **G**). Magnification: ×40 in **A**, ×200 in **F** and **G**, ×400 in **B**, **D**, and **E**, and ×600 in insert in **A**, **C**, insert in **D**, and insert in **E**. Scale bars: 500 μm in **A**, 50 μm in **B**, 20 μm in **C**, and 100 μm in **F**.

*Immunostaining and DC counts*. Mouse kidney, aorta, and lymph nodes were resected, embedded in Tissue-Tek OCT compound (Miles Inc.), snap frozen in liquid nitrogen, and stored at –80°C. Frozen tissues were then sectioned in 5-μm sections, fixed with methanol for 10 minutes at –20°C, and stained with anti-PECAM mAb Mec 13.3 (37) and anti–JAM-A mAb BV12 (1), followed by FITC- or Cy3-conjugated donkey anti-rat Ab's (Jackson ImmunoResearch Laboratories). Frozen lymph nodes were fixed in acetone for 10 minutes at –20°C and double stained with rat anti-mouse JAM-A (BV12) and rabbit anti-mouse LYVE overnight at 4°C, followed by Cy3 donkey anti-rat and FITC goat anti-rabbit Ab's (Jackson ImmuoResearch Laboratories). Fluorescence images of immunostained tissues were analyzed with a Leica DMR fluorescence microscope, and images were recorded with a Hamamatsu 3CCD camera before processing with Adobe Photoshop for Macintosh.

Thin tissue sections from lymph nodes were obtained and stained with H&E for morphological evaluation. For immunofluorescence and immunohistochemistry using an indirect immunoperoxidase technique, lymph nodes and small fragments of mouse ears were embedded and frozen in Tissue-Tek OCT compound. Three-micron sections were air-dried overnight, fixed in acetone for 10 minutes, and incubated with 10% normal rabbit serum. Sections were then incubated with different primary Ab's including rat anti-mouse JAM-A (BV12), anti–MHC class II (clone 2G9, BD Biosciences — Pharmingen), and anti-Langerin (a kind gift of G. Trinchieri, Schering-Plough Corp., Dardilly, France). Primary Ab's were revealed with anti-rat biotinylated secondary Ab's (Vector Laboratories Inc.) followed by Texas red– or FITC-conjugated streptavidin. Slides were mounted in 90% glycerol and analyzed with an Olympus BX60 fluorescence microscope.

Quantitative analysis of epidermal LCs expressing MHC class II was performed by evaluating 30 high-power fields (magnification ×400) obtained from nonconsecutive ear sections. LC numbers were determined by counting MHC class II–positive cells with recognizable stellate morphology and normalizing for the number of basal keratinocytes; data are expressed as mean number of LCs/100 keratinocytes (41).

*Cytokines*. Human CCL3 and CCL19 were from PeproTech Inc. Mouse GM-CSF was from Sandoz Inc. Murine TNF-α was a kind gift from P. Vandenabeele (Gent University, Belgium). Human Flt3 ligand was a generous gift from Immunex Corp. Cytokines were endotoxin free as assessed by Limulus amebocyte assay (BioWhittaker Inc.).

*Chemotaxis and transmigration assays*. Chemotaxis and transendothelial migration experiments were performed in polycarbonate Transwell inserts (5-μm pore, Corning Costar Corp.) as previously described (40), with minor modifications. $^{51}$Cr-labeled DCs ($15 \times 10^4$/well in 0.1 ml for chemotaxis and $5 \times 10^4$/ well in 0.1 ml for transmigration) were seeded in the upper compartment and chemoattractants were placed in the lower compartment. After 90 minutes of incubation at 37°C, the radioactivity present in the lower compartment was evaluated. Chemokines were used at the optimal concentration of 100 ng/ ml. Results are reported as percentage of input, as in the following formula: (cpm in the lower compartment/cpm of the input) × 100. In transmigration experiments, MELCs (38) or the microvascular mouse endothelial cell line 1G11 (40) were grown as monolayers on gelatin- or fibronectin-coated inserts; labeled DCs were applied to the monolayers. In some experiments the MELCs were grown on the upper or lower side of the filter.

*Phagokinetic track assay*. The assay was performed as described (42). Briefly, cells were plated onto glass coverslips previously coated with colloidal gold and incubated for 24 hours at 37°C. Then cells were fixed with 3% paraformaldehyde and observed by light microscopy. Pictures of individual cells were analyzed with NIH Image software for measuring the particle-free area and counting the number of tracks produced by each cell.

In some experiments, BM-DCs from *Jam-A*+/+ mice were incubated during the track assay with anti–JAM-A mAb BV11 (1, 9) and anti-PECAM mAb Mec 13.3 (37) as negative control (20 μg/ml).

*FITC skin painting*. The number of lymph node DCs after FITC skin painting was analyzed as described previously (43). In brief, FITC (Sigma-Aldrich) was dissolved (5 mg/ml) in a 50:50 (vol/vol) acetone-dibutylphthalate mixture just before application. Mice were painted on the shaved abdomen with 0.2 ml of this FITC solution. Inguinal lymph nodes were obtained after 6 hours and 24 hours, mechanically disaggregated, and treated with a mixture of collagenase A (1 mg/ml, Roche Molecular Biochemicals) and DNase (0.4 mg/ml, Roche Molecular Biochemicals) for 30 minutes at 37°C, followed by DNase alone at room temperature for 15 minutes. Cell suspensions were then stained with a PE-labeled hamster anti-mouse CD11c mAb (clone HL3, BD Biosciences — Pharmingen) and PE/FITC double-positive cells were analyzed by FACScan.

*CHS*. CHS was induced and determined as previously described (44). Briefly, the hapten 4-ethoxymethylene-2-phenyl-2-oxazoline-5-one (oxazolone; OXA) (Sigma-Aldrich) was freshly prepared before CHS assays. For sensitization, mice were painted once (day 0) on the shaved abdominal skin with 100 μl of 3% OXA in 4:1 acetone/olive oil (vol/vol) solution. Five days later (day +5) mice were challenged by the application of 10 μl of OXA (1%) on each side of the right ear, while the left ear received the vehicle alone. CHS response was determined by measuring the degree of ear swelling of the antigen-painted ear compared with that of the vehicle-treated contralateral ear at different times after challenge (from 24 to 96 hours) using a dial thickness gauge (Mitutoyo America Corp.). The results were expressed as mean percent of increased swelling calculated over vehicle-treated contralateral ear.

In some experiments CHS was induced by in vivo inoculation of antigen-loaded DCs (45). Cultured BM-DCs were resuspended in HBSS containing 100 μg/ml DNBS (ICN Biomedicals Inc.) and incubated at 37°C for 30 minutes. For sensitization (day 0), $4 \times 10^5$ DNBS-treated DCs (in 200 μl of saline) from *Jam-A*$^{+/+}$ or *Jam-A*$^{-/-}$ mice were injected subcutaneously into the flank of *Jam-A*$^{+/+}$ recipient mice. Five days later, mice were challenged by the application of 10 μl 0.2% 2,4-dinitrofluorobenzene (Sigma-Aldrich) in 4:1 acetone/olive oil solution on each side of the right ear. Some animals were challenged by the application of 10 μl 1% OXA on each side of the right ear, as negative controls. The left ear received vehicle alone. Groups of mice injected with the same number of unmodified DCs, or not injected and challenged with vehicle alone, served as negative controls. CHS response was determined by measuring ear swelling as reported above for OXA.

*Statistical analysis*. Experimental groups included at least five mice. All experiments were performed at least three times. Statistical significance was evaluated using the two-tailed or the paired Student's *t* test, as indicated.

1. Martin-Padura, I., et al. 1998. Junctional adhesion molecule, a novel member of the immunoglobulin superfamily that distributes at intercellular junctions and modulates monocyte transmigration. *J. Cell Biol.* **142**:117–127.
2. Palmeri, D., Van Zante, A., Huang, C.-C., Hemmerich, S., and Rosen, S.D. 2000. Vascular endothelial junction-associated molecule, a novel member of the immunoglobulin superfamily, is localized to intercellular boundaries of endothelial cells. *J. Biol. Chem.* **275**:19139–19145.
3. Aurrand-Lions, M.A., Duncan, L., Ballestrem, C., and Imhof, B.A. 2001. JAM-2, a novel immunoglobulin superfamily molecule, expressed by endothelial and lymphatic cells. *J. Biol. Chem.* **276**:2733–2741.
4. Johnson-Leger, C., Aurrand-Lions, M., and Imhof, B.A. 2000. The parting of the endothelium: miracle, or simply a junctional affair? *J. Cell Sci.* **113**:921–933.
5. Zen, K., and Parkos, C.A. 2003. Leukocyte-epithelial interactions. *Curr. Opin. Cell Biol.* **15**:557–564.
6. Aurrand-Lions, M., Johnson-Leger, C., and Imhof, B.A. 2002. Role of interendothelial adhesion molecules in the control of vascular functions. *Vascul. Pharmacol.* **39**:239–246.
7. Bazzoni, G., et al. 2000. Homophilic interaction of junctional adhesion molecule. *J. Biol. Chem.* **275**:30970–30976.
8. Kostrewa, D., et al. 2001. X-ray structure of junctional adhesion molecule: structural basis for homophilic adhesion via a novel dimerization motif. *EMBO J.* **20**:4391–4398.
9. Del Maschio, A., et al. 1999. Leukocyte recruitment in the cerebrospinal fluid of mice with experimental meningitis is inhibited by an antibody to junctional adhesion molecule (JAM). *J. Exp. Med.* **190**:1351–1356.
10. Ostermann, G., Weber, K.S., Zernecke, A., Schröder, A., and Weber, C. 2002. JAM-1 is a ligand of the beta(2) integrin LFA-1 involved in transendothelial migration of leukocytes. *Nat. Immunol.* **3**:151–158.
11. Ma, S., et al. 2003. Dynamics of junctional adhesion molecule 1 (JAM1) during leukocyte transendothelial migration under flow in vitro. Experimental Biology Meeting, abstract 2712. *FASEB J.* **17**:A1189.
12. Steinman, R.M. 1991. The dendritic cell system and its role in immunogenicity. *Annu. Rev. Immunol.* **9**:271–296.
13. Sakai, K., and Miyazaki, J. 1997. A transgenic mouse line that retains Cre recombinase activity in mature oocytes irrespective of the cre transgene transmission. *Biochem. Biophys. Res. Commun.* **237**:318–324.
14. Cattelino, A., et al. 2003. The conditional inactivation of beta-catenin gene in endothelial cells causes a defective vascular pattern and increased vascular fragility. *J. Cell Biol.* **162**:1111–1122.
15. Elson, D.A., et al. 2001. Induction of hypervascularity without leakage or inflammation in transgenic mice overexpressing hypoxia-inducible factor-1alpha. *Genes Dev.* **15**:2520–2532.
16. Kisanuki, Y.Y., et al. 2001. Tie2-Cre transgenic mice: a new model for endothelial cell-lineage analysis in vivo. *Dev. Biol.* **230**:230–242.
17. Forster, R., et al. 1999. CCR7 coordinates the primary immune response by establishing functional microenvironments in secondary lymphoid organs. *Cell.* **99**:23–33.
18. Gunn, M.D., et al. 1999. Mice lacking expression of secondary lymphoid organ chemokine have defects in lymphocyte homing and dendritic cell localization. *J. Exp. Med.* **189**:451–460.
19. Karkkainen, M.J., Makinen, T., and Alitalo, K. 2002. Lymphatic endothelium: a new frontier of metastasis research. *Nat. Cell Biol.* **4**:E2–E5.
20. Oliver, G., and Detmar, M.T. 2002. The rediscovery of the lymphatic system: old and new insights into the development and biological function of the lymphatic vasculature. *Genes Dev.* **16**:773–783.
21. Skobe, M., and Detmar, M. 2000. Structure, function, and molecular control of the skin lymphatic system. *J. Investig. Dermatol. Symp. Proc.* **5**:14–19.
22. Bazzoni, G., et al. 2000. Interaction of junctional adhesion molecule with the tight junction components ZO-1, cingulin, and occludin. *J. Biol. Chem.* **275**:20520–20526.
23. Martinez-Estrada, O.M., et al. 2001. Association of junctional adhesion molecule with calcium/calmodulin-dependent serine protein kinase (CASK/LIN-2) in human epithelial caco-2 cells. *J. Biol. Chem.* **276**:9291–9296.
24. Ebnet, K., et al. 2000. Junctional adhesion molecule interacts with the PDZ domain-containing proteins AF-6 and ZO-1. *J. Biol. Chem.* **275**:27979–27988.
25. Ebnet, K., et al. 2001. The cell polarity protein ASIP/PAR-3 directly associates with junctional adhesion molecule (JAM). *EMBO J.* **20**:3738–3748.
26. Ohno, S. 2001. Intercellular junctions and cellular polarity: the PAR-aPKC complex, a conserved core cassette playing fundamental roles in cell polarity. *Curr. Opin. Cell Biol.* **13**:641–648.
27. Fanning, A.S., Ma, T.Y., and Anderson, J.M. 2002. Isolation and functional characterization of the actin binding region in the tight junction protein ZO-1. *FASEB J.* **16**:1835–1837.
28. Boettner, B., Govek, E.E., Cross, J., and Van Aelst, L. 2000. The junctional multidomain protein AF-6 is a binding partner of the Rap1A GTPase and associates with the actin cytoskeletal regulator profilin. *Proc. Natl. Acad. Sci. U. S. A.* **97**:9064–9069.
29. Cohen, A.R., et al. 1998. Human CASK/LIN-2 binds syndecan-2 and protein 4.1 and localizes to the basolateral membrane of epithelial cells. *J. Cell Biol.* **142**:129–138.
30. Eickholt, B.J., Walsh, F.S., and Doherty, P. 2002. An inactive pool of GSK-3 at the leading edge of growth cones is implicated in Semaphorin 3A signaling. *J. Cell Biol.* **157**:211–217.
31. Muller, W.A. 2003. Leukocyte–endothelial-cell

interactions in leukocyte transmigration and the inflammatory response. *Trends Immunol.* **24**:326–333.

32. Allavena, P., Dejana, E., Bussolino, F., Vecchi, A., and Mantovani, A. 1995. Cytokine regulation of endothelial cells. In *Cytokines*. F.R. Balkwill, editor. Oxford University Press. New York, New York, USA. 225–245.

33. Bussolino, F., et al. 1991. Murine endothelioma cell lines transformed by polyoma middle T oncogene as target for and producers of cytokines. *J. Immunol.* **147**:2122–2129.

34. Anfosso, F., et al. 2001. Outside-in signaling pathway linked to CD146 engagement in human endothelial cells. *J. Biol. Chem.* **276**:1564–1569.

35. Balconi, G., Spagnuolo, R., and Dejana, E. 2000. Development of endothelial cell lines from embryonic stem cells. A tool for studying genetically manipulated endothelial cells in vitro. *Arterioscler. Thromb. Vasc. Biol.* **20**:1443–1451.

36. Corada, M., et al. 1999. Vascular endothelial-cadherin is an important determinant of microvascular integrity in vivo. *Proc. Natl. Acad. Sci. U. S. A.* **96**:9815–9820.

37. Vecchi, A., et al. 1994. Monoclonal antibodies specific for endothelial cells of mouse blood vessels. Their application in the identification of adult and embrionic endothelium. *Eur. J. Cell Biol.* **63**:247–254.

38. Fra, A.M., et al. 2003. Scavenging of inflammatory CC chemokines by the promiscuous putatively silent chemokine receptor D6. *J. Immunol.* **170**:2279–2282.

39. Valiron, O., et al. 1996. Desmoplakin expression and organization at human umbilical vein endothelial cell-to-cell junctions. *J. Cell Sci.* **109**:2141–2149.

40. Vecchi, A., et al. 1999. Differential responsiveness to constitutive vs. inducible chemokines of immature and mature mouse dendritic cells. *J. Leukoc. Biol.* **66**:489–494.

41. Bauer, J., et al. 2001. A strikingly constant ratio exists between Langerhans cells and other epidermal cells in human skin. A stereologic study using the optical disector method and the confocal laser scanning microscope. *J. Invest. Dermatol.* **116**:313–318.

42. Albrecht-Buehler, G. 1977. The phagokinetic tracks of 3T3 cells. *Cell.* **11**:395–404.

43. Macatonia, S.E., Knight, S.C., Edwards, A.J., Griffiths, S., and Fryer, P. 1987. Localization of antigen on lymph node dendritic cells after exposure to the contact sensitizer fluorescein isothiocyanate. Functional and morphological studies. *J. Exp. Med.* **166**:1654–1667.

44. Wang, B., et al. 1997. Depressed Langerhans cell migration and reduced contact hypersensitivity response in mice lacking TNF receptor p75. *J. Immunol.* **159**:6148–6155.

45. Krasteva, M., et al. 1998. Dual role of dendritic cells in the induction and down-regulation of antigen-specific cutaneous inflammation. *J. Immunol.* **160**:1181–1190.